Electronic Supplementary Material (ESI) for Chemical Communications.

Supporting Information for

Accessing the inaccessible: discrete multinuclear coordination complexes and selective anion binding attainable only by tethering ligands together

Basil M. Ahmed and Gellert Mezei*

Department of Chemistry, Western Michigan University, Kalamazoo, Michigan, USA

*Correspondent author. Email: gellert.mezei@wmich.edu

CONTENTS **PAGE**

1. MATERIALS AND METHODS

All reagents and solvents are commercially available and are used as received. THF is inhibited with 250 ppm BHT. Diethyl ether is dried by distillation from Na/benzophenone.

Mass spectrometric analyses are performed on a Waters Synapt G1 HDMS instrument, using electrospray ionization (ESI). Sample solutions (10^{-4}–10^{-5} M in CH_3CN) are infused by a syringe pump at 5 μL/min and nitrogen is supplied as nebulizing gas at 500 L/h. The electrospray capillary voltage is set to –2.5 or +3.0 kV, respectively, with a desolvation temperature of 110 °C. The sampling and extraction cones are maintained at 40 V and 3.0 V, respectively, at 80 °C. NMR spectra are collected on a Jeol JNM-ECP400 instrument. For variable-temperature measurements, temperatures are measured using an ethylene glycol standard. UV−vis measurements are carried out on a Shimadzu UV-1650PC spectrophotometer. Thermogravimetric analysis is performed on a TA Instruments Model Q500 analyzer.

2. SYNTHESIS

2.1. Synthesis of 1,2-bis(1*H*-pyrazole-3-yl)ethane (LH_2).

Method A.

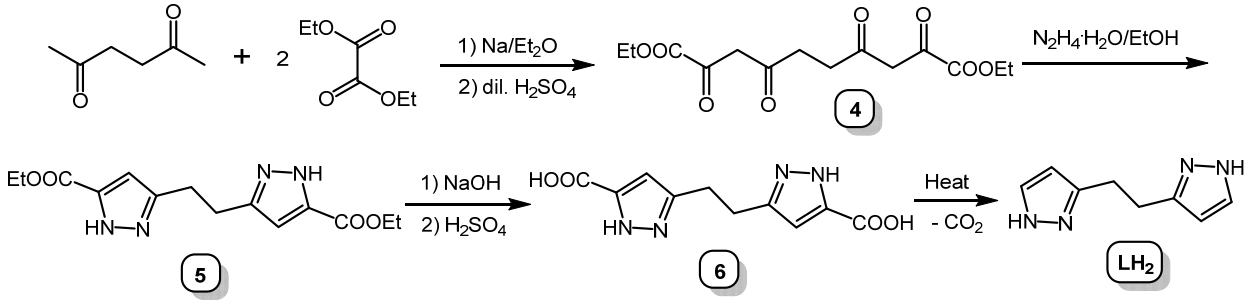

*a) Synthesis of diethyl 2,4,7,9-tetraoxodecanedione (**4**).* Sodium metal (small pieces, 11.500 g, 500 mmol) is placed into a 1000 ml three-necked round bottom flask equipped with a stir-bar, condenser and addition funnel, and connected to a Schlenk line. After evacuation and purging with N_2, the flask is placed into an ice bath and anhydrous diethyl ether (500 ml) is added by syringe. A mixture of diethyl oxalate (73.000 g, 500 mmol) and 2,5-hexanedione (28.500 g, 250 mmol) is slowly added under stirring, and the dark brown suspension is further stirred for 2 hours at 0 °C. After warming up to room temperature overnight under an N_2 atmosphere, the

reaction mixture is refluxed for 1 hour. The brown suspension is filtered out, washed with diethyl ether, and dried under high vacuum. The solid is then dissolved in deionized water (2 L) and acidified to pH ~ 3 with a 10% aqueous solution of H_2SO_4 (200 mL). A light yellowish-brown precipitate forms, which is filtered out and dried under high vacuum (22.310 g). Recrystallization from hot ethanol affords 14.593 g (19%) of **4**, as shiny, brownish plates. NMR in $CDCl_3$ shows the pure enolic form. ^{1}H NMR (400 MHz, $CDCl_3$): δ 6.43 (s, 2H, COC*H*COH), 4.34 (q, 4H, ^3J = 7.2 Hz, CH_3CH_2), 2.91 (s, 4H, $COCH_2CH_2CO$), 1.36 (t, 6H, ^3J = 7.1 Hz, CH_3CH_2) ppm. ^{13}C NMR (101 MHz, $CDCl_3$): δ 202.5, 163.4, 162.0, 102.5, 62.7, 35.3, 14.1 ppm.

*b) Synthesis of 1,2-bis(5-carboethoxy-1H-pyrazole-3-yl)ethane (**5**).* To a hot solution of compound **4** (14.000 g, 44.5 mmol) in 100 ml ethanol is gradually added hydrazine hydrate (5.05 g, 4.90 mL, 100 mmol). A crystalline solid forms, which is stirred for 30 minutes, filtered, re-crystallized from hot ethanol and dried under vacuum to give **5** (10.215 g, 75%) as a light brown microcrystalline powder. ^{1}H NMR (400 MHz, DMSO-d_6): δ 6.52 (s, 2H, pz-*H*), 4.24 (q, 4H, ^3J = 7.1 Hz, CH_3CH_2), 2.97 (s, 4H, CH_2CH_2), 1.27 (t, 6H, ^3J = 7.2 Hz, CH_3CH_2) ppm. ^{13}C NMR (101 MHz, DMSO-d_6): δ 162.0, 145.6, 142.0, 106.7, 60.6, 25.4, 14.8 ppm.

*c) Synthesis of 1,2-bis(5-carboxy-1H-pyrazol-3-yl)ethane (**6**).* Compound **5** (10.000 g, 32.6 mmole) is dissolved in a 10% aqueous NaOH solution (100 mL) and is boiled for 1 hour. After cooling, a 20% aqueous H_2SO_4 solution (40 mL) is added gradually, under stirring, to pH~3). The brown precipitate is filtered out, suspended in 37% HCl (250 mL) and boiled for 30 minutes. Filtration and drying in high vacuum affords 6.528 g (80%) of **6** as a beige powder. ^{1}H NMR (400 MHz, DMSO-d_6): δ 6.48 (s, 2H, pz-*H*), 2.95 (s, 4H, CH_2CH_2) ppm. ^{13}C NMR (101 MHz, DMSO-d_6): δ 163.0, 146.9, 141.1, 106.8, 25.8 ppm.

*d) Synthesis of 1,2-bis(1H-pyrazol-3-yl)ethane (**LH_2**).* Compound **6** (4.66 g, 18.62 mmole) is added to a vial preheated to 330 °C in a sand bath covered with a watch glass. As the material starts melting, a white smoke is evolved which condenses onto the watch glass. After all the material has melted, the vial is taken out of the sand bath and left to cool to room temperature. The white solid condensed onto the watch glass (~ 50 mg) is pure **LH_2**. The dark brown molten residue is extracted with boiling ethanol under stirring. After filtration, the ethanolic extract is heated and stirred for 2 hours with activated carbon, then filtered and evaporated to give a yellowish-brown oil (1.5 g). Upon trituration with diethyl ether, pure **LH_2** is obtained as a pale yellow powder (900 mg; overall yield: 32%). ^{1}H NMR (400 MHz, DMSO-d_6): δ 12.48 (s, 2H,

N*H*), 7.45 (s, 2H, 5-*H*-pz), 6.03 (s, 2H, 4-*H*-pz), 2.88 (s, 4H, CH_2CH_2) ppm (Fig. S3). ^{13}C NMR (101 MHz, DMSO-d_6): δ 147.1, 134.0, 103.4, 26.9 ppm (Fig. S4). HRMS (ESI-TOF) *m/z*: $[M+Na]^+$ calcd. for $C_8H_{10}N_4Na$ 185.0803; found 185.0808. Slow evaporation of an EtOH/H_2O solution of **LH_2** produces single-crystals suitable for X-ray diffraction (see Table S1 and Figs. S18 and S19).

Method B.

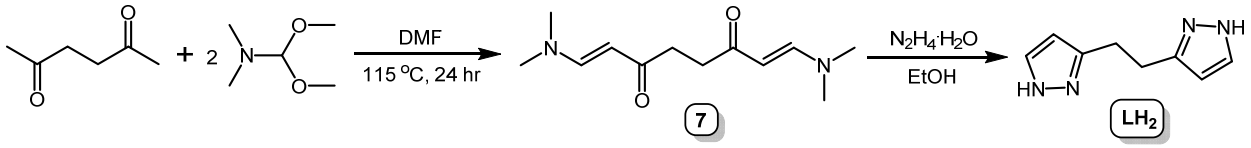

*a) Synthesis of (1E, 7E)-1,8-bis(dimethylamino)octa-1,7-diene-3,6-dione (**7**).* A solution of 2,5-hexanedione (10.00 g, 0.0876 mol) and dimethylformamide dimethylacetal (81.45 mL, 73.07 g, 0.613 mol) in dimethylformamide (100 mL) is refluxed in a 250 mL round-bottom flask at 115 ºC for 24 hours. The color of the solution gradually turns yellow and finally dark red. The excess DMF-DMA and the DMF solvent are distilled out under high-vacuum with heating on a water bath (at ~60 °C). The viscous, dark-red oily residue (20.129 g) is purified by column chromatography on silica gel (1.5 kg) using EtOAc/MeOH gradient elution (first 9:1, then 8:2, 7:3, 2:1 and 1:1). R_f is 30% with EtOAc:MeOH (2:1) and 7% with EtOAc:MeOH (9:1). Compound **7** is obtained as a brown solid (yield: 4.183 g, 21%). Further purification can be carried out by recrystallization from an ethyl acetate solution by hexane vapor diffusion, which affords single crystals suitable for X-ray diffraction (see Table S1 and Fig. S17). ^{1}H NMR (400 MHz, $CDCl_3$): δ 7.49 (d, 2H, ^3J = 13 Hz, =C*H*), 5.05 (d, 2H, ^3J = 13 Hz, =C*H*), 2.79–3.00 (m, 12H, N(CH_3)$_2$), 2.64 (s, 4H, CH_2CH_2) ppm (Fig. S1). ^{13}C NMR (101 MHz, $CDCl_3$): δ 197.2, 152.5, 96.1, 44.8, 37.0, 36.2 ppm (Fig. S2). HRMS (ESI-TOF) *m/z*: $[M+Na]^+$ calcd. for $C_{12}H_{10}N_2NaO_2$ 247.1422; found 247.1427.

*b) Synthesis of 1,2-bis(1H-pyrazole-3-yl)ethane (**LH_2**).* Compound **7** (1.000 g, 4.45 mmole) is dissolved in ethanol (50 mL) and hydrazine monohydrate (0.54 mL, 0.56 g, 11 mmole) is added. After refluxing for 6 hours, a brown precipitate is filtered out. The dark brown filtrate is stirred with activated carbon for 30 minutes with heating, and then is filtered while hot. The solvent is removed under vacuum and ligand **LH_2** is obtained as a light yellow solid (yield: 0.656 g, 91%).

2.2. Synthesis of $Cu_4(OH)_2(L)_2(NO_3)_2(H_2O)_2(THF)$.

$Cu(NO_3)_2{\cdot}2.5H_2O$ (860 mg, 3.70 mmol), 1,2-bis(1*H*-pyrazol-3-yl)ethane (**LH_2**) (300 mg, 1.85 mmol) and NaOH (222 mg, 5.55 mmol) are stirred in 30 ml THF for 3 days. A brown solid is removed from the dark blue solution by filtration and the solvent is evaporated in vacuum. A dark blue solid is obtained. Yield: 700 mg (90%). Anal. Calcd for $C_{20}H_{30}Cu_4N_{10}O_{11}$: C, 28.57; H, 3.60; N, 16.66. Found: C, 28.98; H, 3.54; N, 16.38. ^{1}H NMR (400 MHz, 25 °C, DMSO-d_6): δ 132.39 (s, br, O*H*), 52.07 (s, br, 4H, *H*-pz), 46.05 (s, br, 4H, *H*-pz), 3.55 (s, br, *H*-THF, H_2O), 1.72 (s, br, 4H, *H*-THF), −0.22 (s, br, 4H, CH_2CH_2), −2.40 (s, br, 4H, CH_2CH_2) ppm.

In the ESI-MS(−) spectrum of **1**$(H_2O)_2$(THF) in CH_3CN, the base peak observed at *m/z* 730.7 corresponds to $[Cu_4O(OH)(L)_2(NO_3)_2]^-$. Other peaks, corresponding to $[Cu_4(OH)_4(L)_2(NO_3)]^-$ (*m/z* 703.7), $[Cu_4O_2(L)_2(NO_3)]^-$ (*m/z* 667.8), $[Cu_4O(OH)_3(L)_2]^-$ (*m/z* 640.8), and dimeric $[Cu_8O(OH)_3(L)_4(NO_3)_4]^-$ (*m/z* 1462.5), $[Cu_8O_2(OH)(L)_4(NO_3)_4]^-$ (*m/z* 1444.5), $[Cu_8(OH)_6(L)_4(NO_3)_3]^-$ (*m/z* 1435.5), $[Cu_8O(OH)_4(L)_4(NO_3)_3]^-$ (*m/z* 1417.6), $[Cu_8O_2(OH)_2(L)_4(NO_3)_3]^-$ (*m/z* 1399.6), $[Cu_8O_3(L)_4(NO_3)_3]^-$ (*m/z* 1381.5), $[Cu_8O_2(OH)_3(L)_4(NO_3)_2]^-$ (*m/z* 1354.5) and $[Cu_8O_3(OH)(L)_4(NO_3)_2]^-$ (*m/z* 1336.6), are also observed. In the ESI-MS(+) spectrum, the base peak observed at *m/z* 606.8 corresponds to $[Cu_4O(OH)(L)_2]^+$. Other peaks, corresponding to $[Cu_8(OH)_4(L)_4(NO_3)_3]^+$ (*m/z* 1401.7), $[Cu_4(OH)_3(L)_2]^+$ (*m/z* 624.8) and $[Cu_3(OH)_2(L)(NO_3)]^+$ (*m/z* 446.9), are also observed.

2.3. Synthesis of $(Bu_4N)[Cu_4(OH)(L)_4]$.

Method A. $Cu_4(OH)_2(L)_2(NO_3)_2(H_2O)_2$(THF) (200 mg, 0.238 mmol), 1,2-bis(1*H*-pyrazol-3-yl)ethane (**LH_2**) (77.2 mg, 0.476 mmol), NaOH (19.0 mg, 0.475 mmol) and Bu_4NOH (1 M in H_2O) (238 mg, 0.238 mmol) are stirred in 20 ml THF for 2 days. The deep violet solution is filtered and the solid residue is rinsed with CH_2Cl_2 (part of the product is not soluble in THF). The solvent is evaporated and the dark violet solid is recrystallized from CH_2Cl_2 by Et_2O vapor diffusion. Yield: 213 mg (81%). Anal. Calcd for $C_{48}H_{69}Cu_4N_{17}O$: C, 49.94; H, 6.03; N, 20.63. Found: C, 49.82; H, 6.42; N, 20.76. ESI-MS(−): *m/z* 911.0.

Method B. $Cu(NO_3)_2{\cdot}2.5H_2O$ (143 mg, 0.615 mmol), 1,2-bis(1*H*-pyrazol-3-yl)ethane (**LH_2**) (100 mg, 0.616 mmol), NaOH (49 mg, 1.2 mmol) and Bu_4NOH (1 M in H_2O) (156 mg, 0.154 mmol) are stirred in 20 ml THF for 2 days. A beige solid is removed from the deep violet solution by filtration and the solvent is evaporated to yield 177 mg dark violet powder (yield: 99%).

2.4. Synthesis of $(Bu_4N)_2[CO_3^{2-}\subset\{Cu^{II}_n(OH)_n(L)_{n/2}\}]$ (n = 26, 28, 30).

Method A. $Cu_4(OH)_2(L)_2(NO_3)_2(H_2O)_2(THF)$ (200 mg, 0.238 mmol), NaOH (16.3 mg, 0.408 mmol), Bu_4NOH (1 M in H_2O) (68.0 mg, 0.0680 mmol) and $Na_2CO_3 \cdot H_2O$ (4.2 mg, 0.034 mmol) are stirred in 20 ml THF for 2 days. The dark blue solution is filtered and the solvent is removed in vacuum. The residue is triturated with Et_2O, filtered, rinsed with Et_2O and dried in vacuum. Yield: 155 mg (~90%). ESI-MS(−) in acetonitrile solution indicates that the product contains $[CO_3\subset\{Cu^{II}_{26}(OH)_{26}(L)_{13}\}]^{2-}$ (*m/z* 2117.6), $[CO_3\subset\{Cu^{II}_{28}(OH)_{28}(L)_{14}\}]^{2-}$ (*m/z* 2278.5), $[CO_3\subset\{Cu^{II}_{28}(OH)_{27}(L)_{14}(LH)\}]^{2-}$ (*m/z* 2350.1) and $[CO_3\subset\{Cu^{II}_{30}(OH)_{30}(L)_{15}\}]^{2-}$ (*m/z* 2439.0).

Method B. $Cu(NO_3)_2 \cdot 2.5H_2O$ (287 mg, 1.23 mmol), 1,2-bis(1*H*-pyrazol-3-yl)ethane (**LH_2**) (100 mg, 0.616 mmol) and Bu_4NOH (55% in H_2O) (1.217 g, 2.555 mmol) are stirred in 20 ml THF for 2 days. The deep-blue solution is filtered (light brown solid) into H_2O (200 mL) under vigorous stirring. The blue precipitate is filtered off, washed thoroughly with water and dried in vacuum. Yield: 196 mg (~88%).

Method C. 143 mg $Cu(NO_3)_2 \cdot 2.5H_2O$ (0.615 mmol), 48.0 mg NaOH (1.20 mmol), 50.0 mg 1,2-bis(1*H*-pyrazol-3-yl)ethane (**LH_2**) (0.308 mmol), 2.7 mg $Na_2CO_3 \cdot H_2O$ (0.022 mmol) and 44 mg Bu_4NOH (1M in H_2O; 0.044 mmol) are added to 10 ml THF, and the mixture is stirred for 4 days. A dark brown-grey solid is removed from the deep blue solution by filtration and the solvent is evaporated to yield 112 mg dark blue powder. Purification is carried out by redissolving in THF and precipitation with H_2O, as described above.

Method D. The synthesis described above (Method C) is repeated with $CuSO_4 \cdot 5H_2O$ (154 mg, 0.617 mmol) instead of $Cu(NO_3)_2 \cdot 2.5H_2O$ and without $Na_2CO_3 \cdot H_2O$. In contrast to the previous experiment, there is no apparent reaction after 4 days. After three weeks, however, as CO_2 from air is gradually absorbed by the reaction mixture, a blue solution forms. Electrospray ionization mass spectrometry indicates that the same carbonate-encapsulating nanojar mixture forms as before, when carbonate is deliberately added from the beginning, and no sulfate-encapsulating nanojars can be detected by ESI-MS.

3. NMR DATA

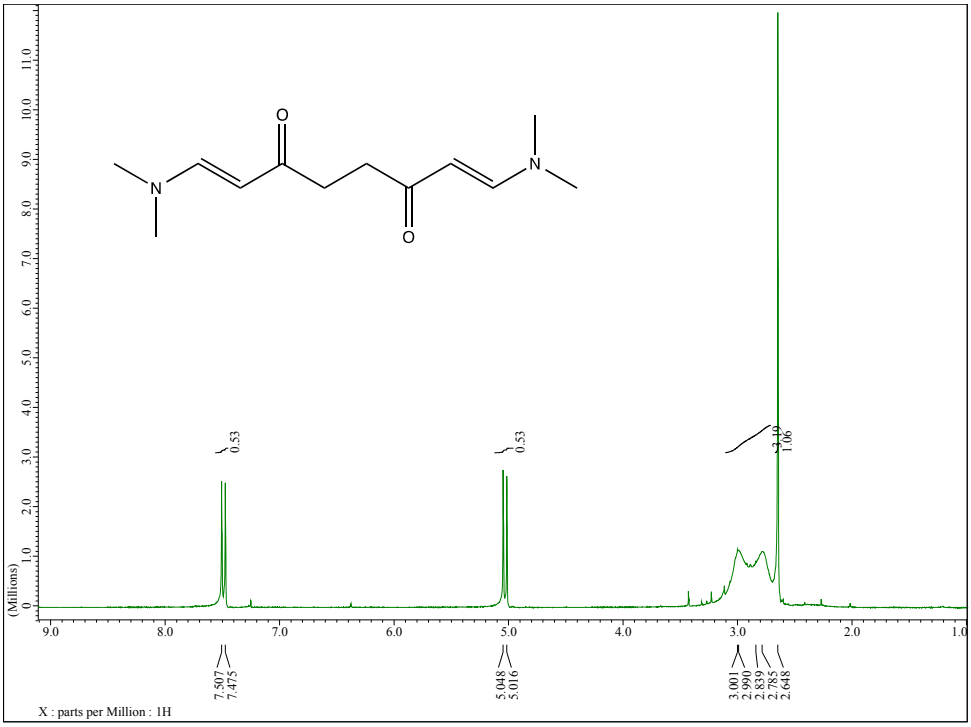

Figure S1. ^{1}H NMR spectrum (400 MHz, $CDCl_3$) of compound **7**.

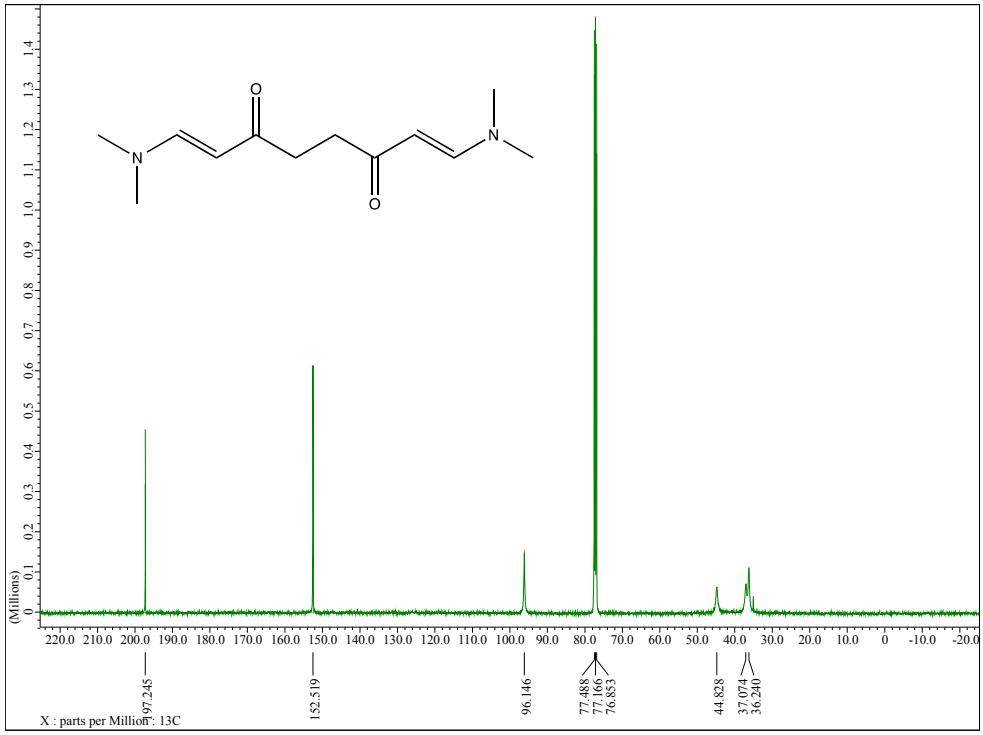

Figure S2. ^{13}C NMR spectrum (101 MHz, $CDCl_3$) of compound **7**.

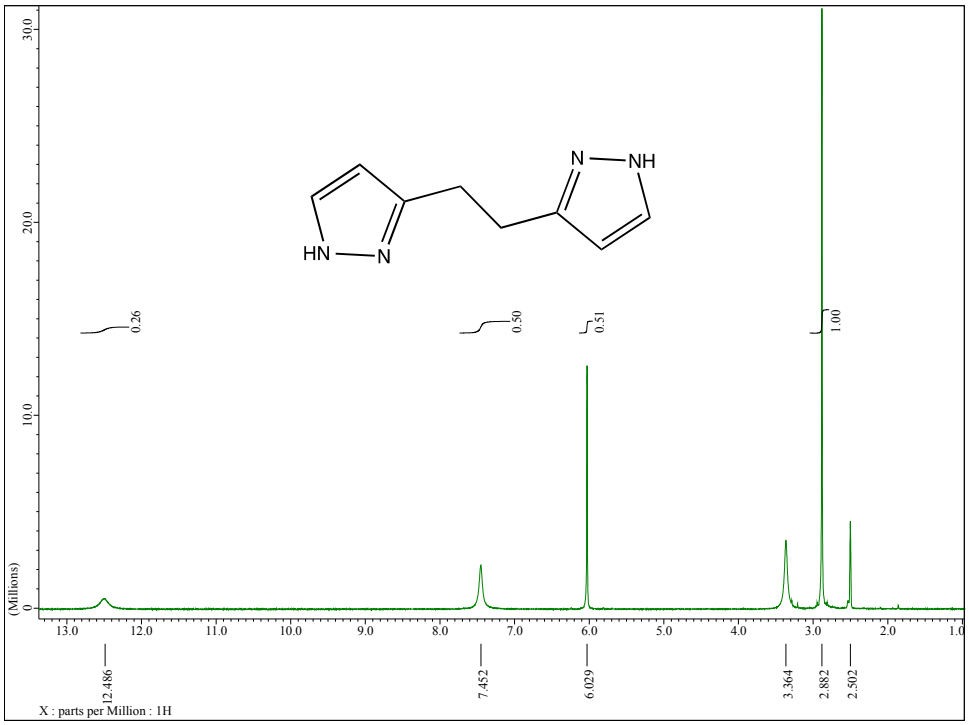

Figure S3. ^{1}H NMR spectrum (400 MHz, DMSO-d_6) of ligand $\mathbf{LH_2}$.

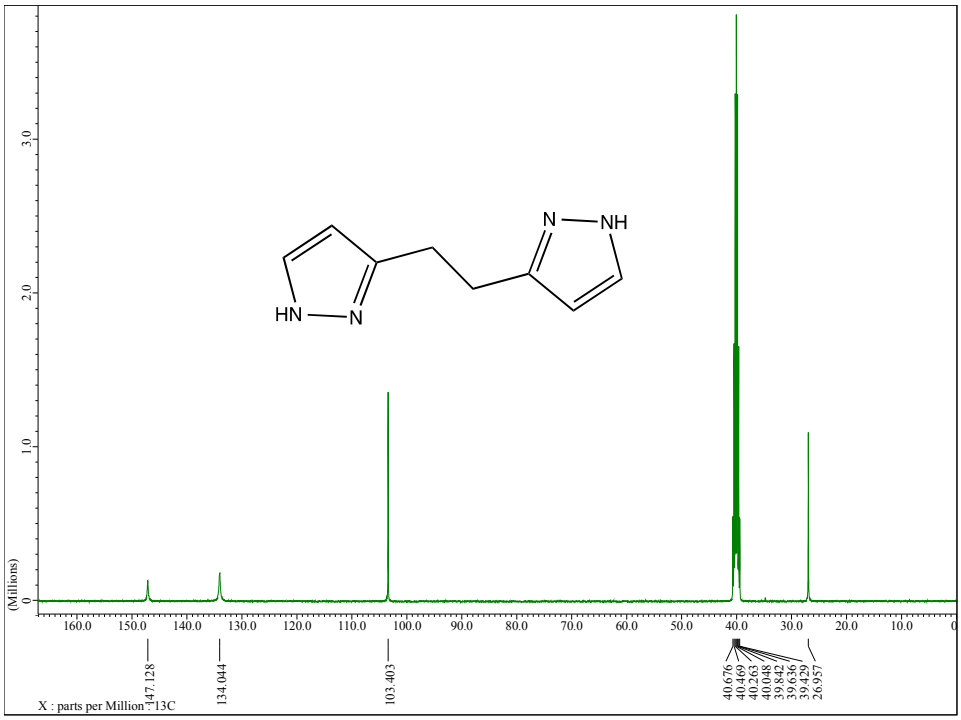

Figure S4. ^{13}C NMR spectrum (101 MHz, DMSO-d_6) of ligand $\mathbf{LH_2}$.

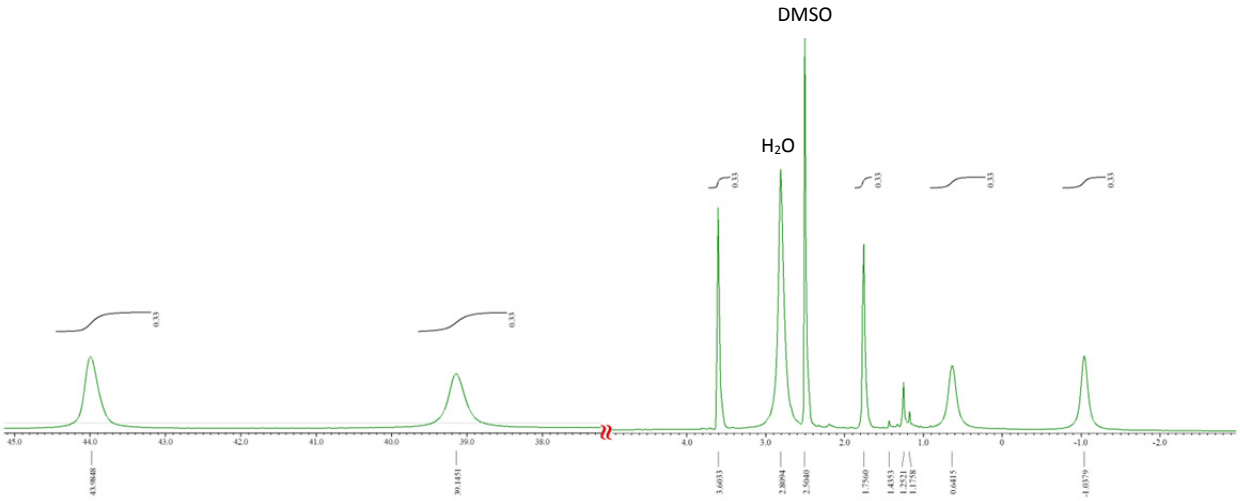

Figure S5. ^{1}H NMR spectrum (400 MHz, DMSO-d_6, 150 °C) of **1**$(H_2O)_2$(THF), showing the 1:1 stoichiometry between complex **1** and THF.

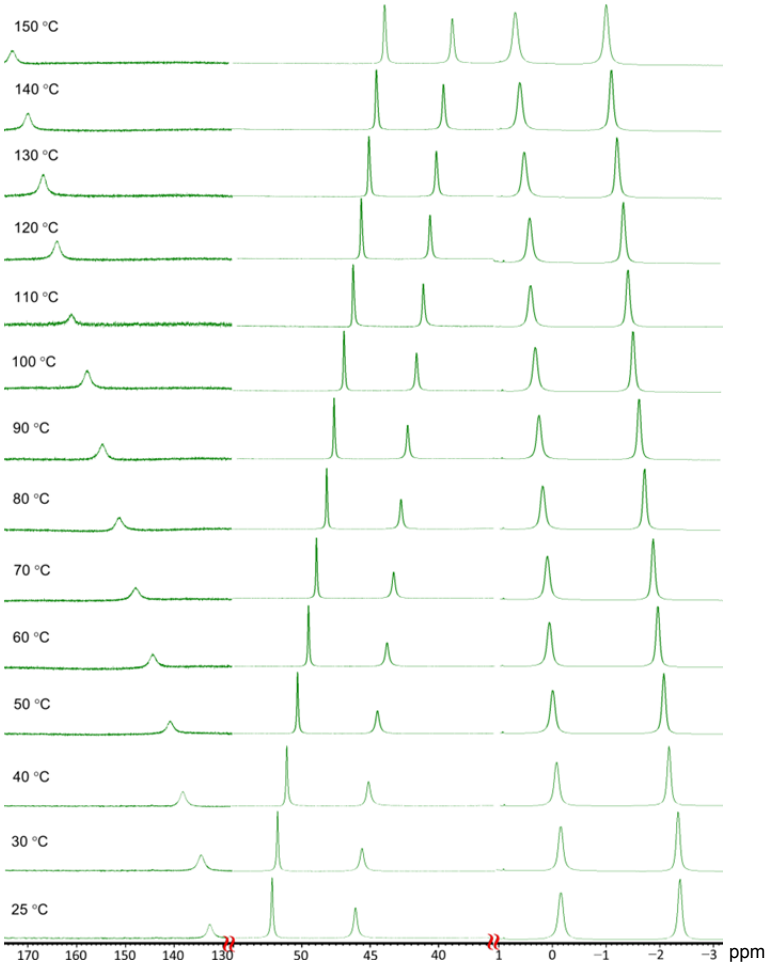

Figure S6. Variable-temperature ^{1}H NMR spectra (in DMSO-d_6) of [$Cu_4(\mu_3$-OH)$(\mu_3$-L$)_2(NO_3)_2(H_2O)_2$(THF)] (**1**). Only the regions between 125−175 ppm (OH proton), 35−55 pm (pz protons) and (−3)−1 ppm (CH_2CH_2 protons) are shown for clarity.

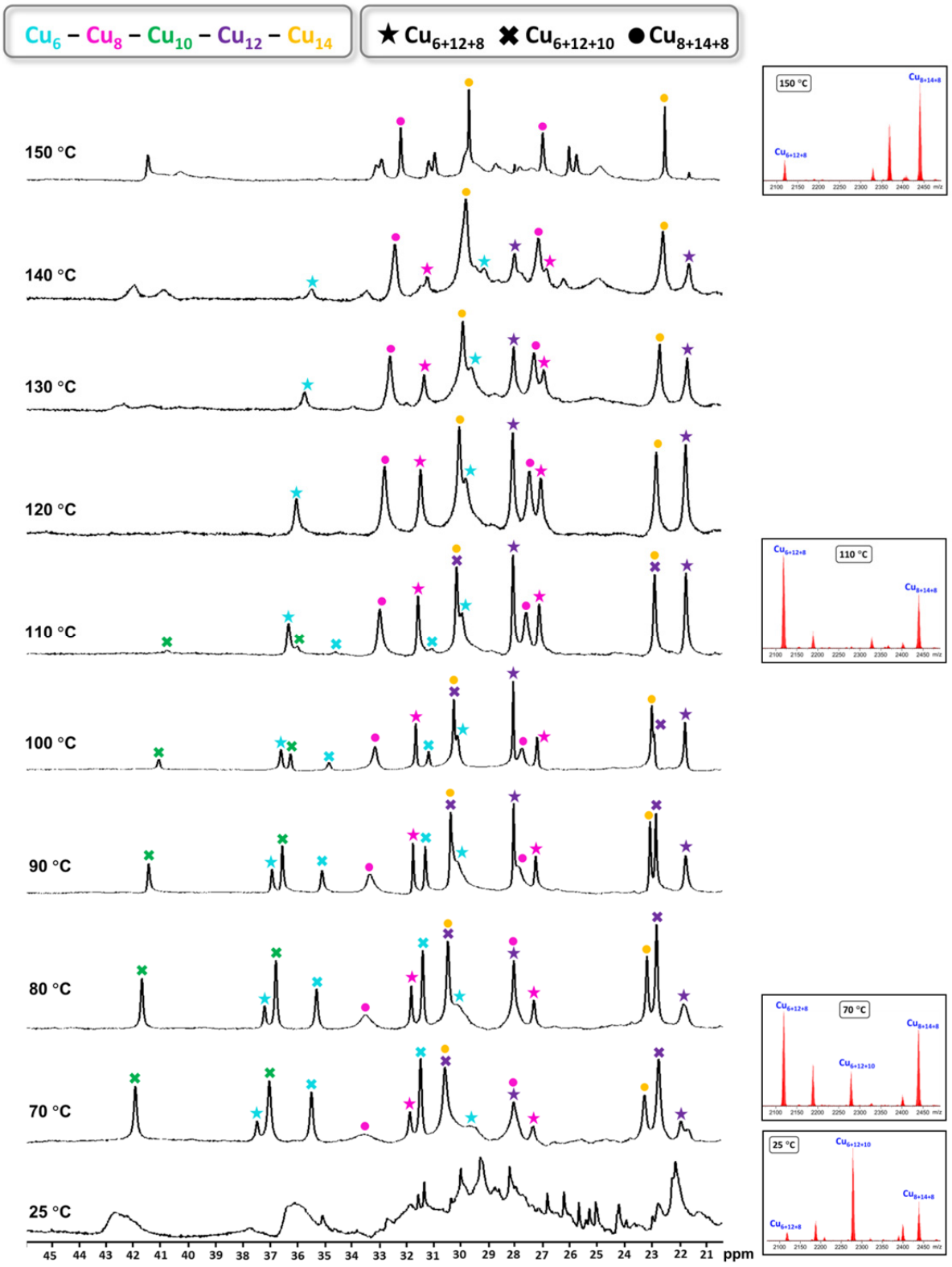

Figure S7. Variable-temperature ^{1}H NMR spectra (in DMSO-d_6) of the mixture of nanojars with ligand L (pyrazole signals in the 21−45 ppm window). See figures S12−S15 for the full ESI-MS spectra.

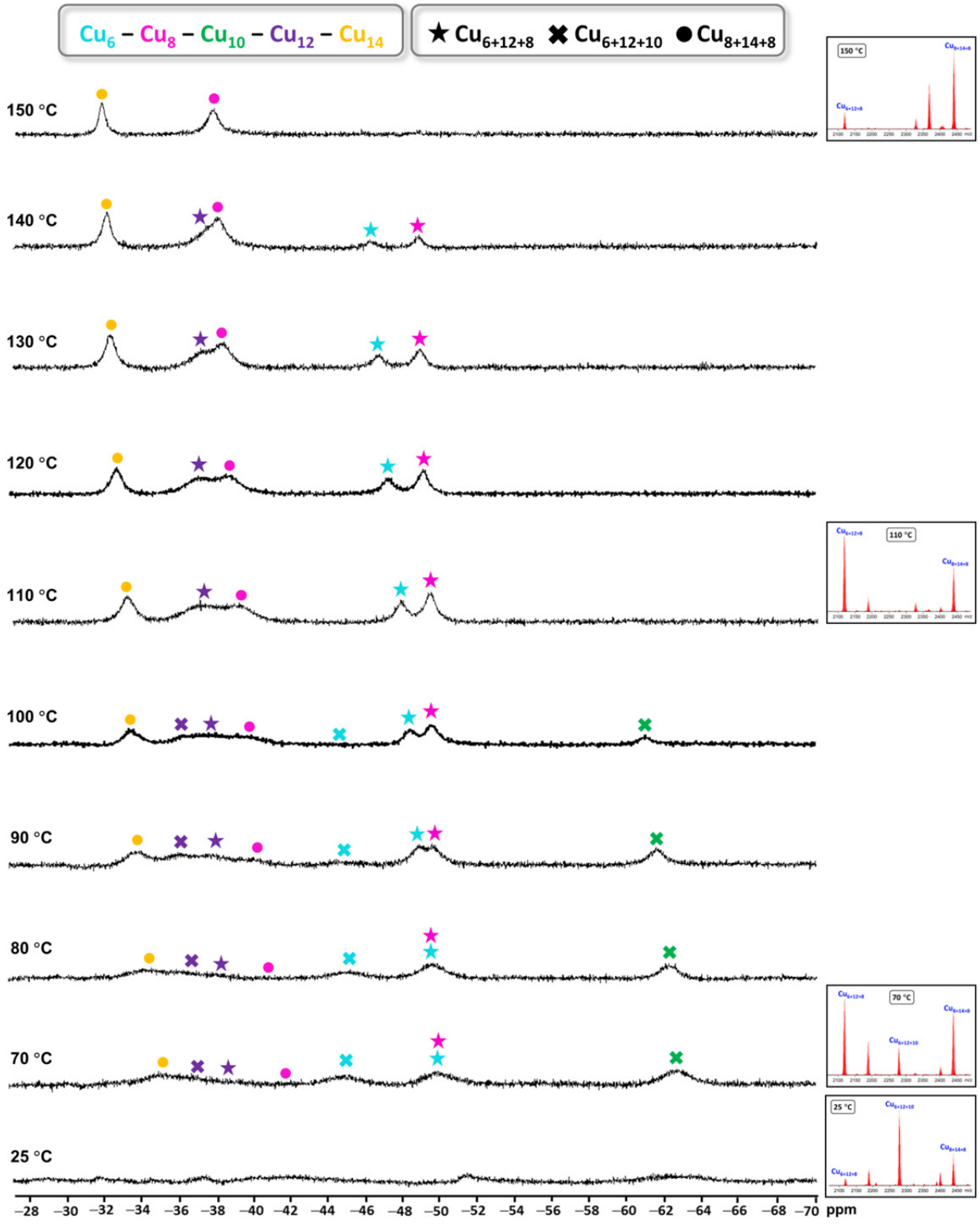

Figure S8. Variable-temperature ^{1}H NMR spectra (in DMSO-d_6) of the mixture of nanojars with ligand L (OH signals in the (−28)−(−70) ppm window). See figures S12−S15 for the full ESI-MS spectra.

4. UV-VIS DATA

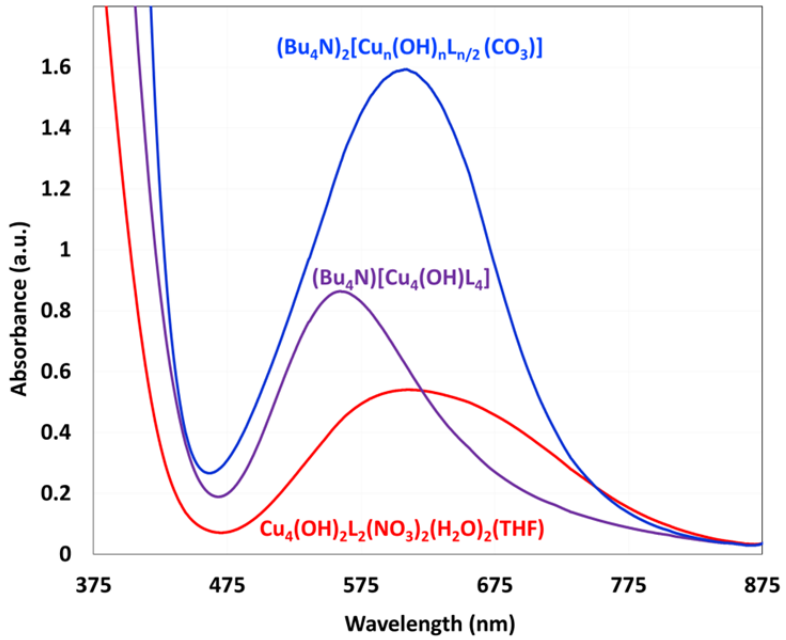

Figure S9. UV-vis spectra of the tetranuclear complexes **1** (red line) and **2** (violet line) (2.600×10^{-3} M in CH_2Cl_2), and the mixture of nanojars containing **3** (blue line) (6.500×10^{-4} M in CH_2Cl_2).

5. THERMOGRAVIMETRIC DATA

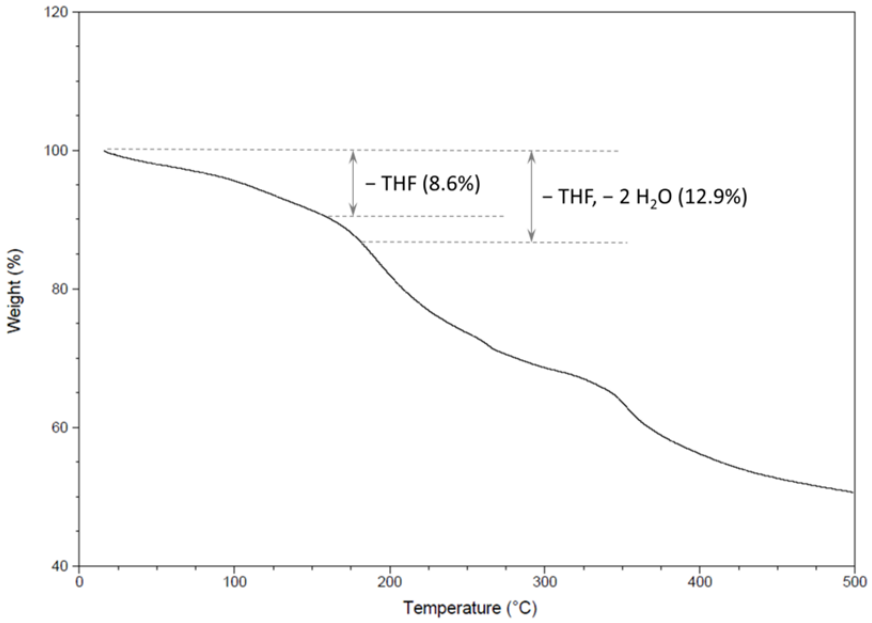

Figure S10. Thermogravimetric curve of $Cu_4(\mu_3\text{-}OH)_2(\mu_3\text{-}L)_2(NO_3)_2(H_2O)_2(THF)$, heated at 3 °C/min under N_2. Calculated loss of the THF molecule: 8.58%; observed: 8.6%. Calculated loss of the THF and the two H_2O molecules: 12.86%; observed: 12.9%.

6. MASS SPECTROMETRIC DATA

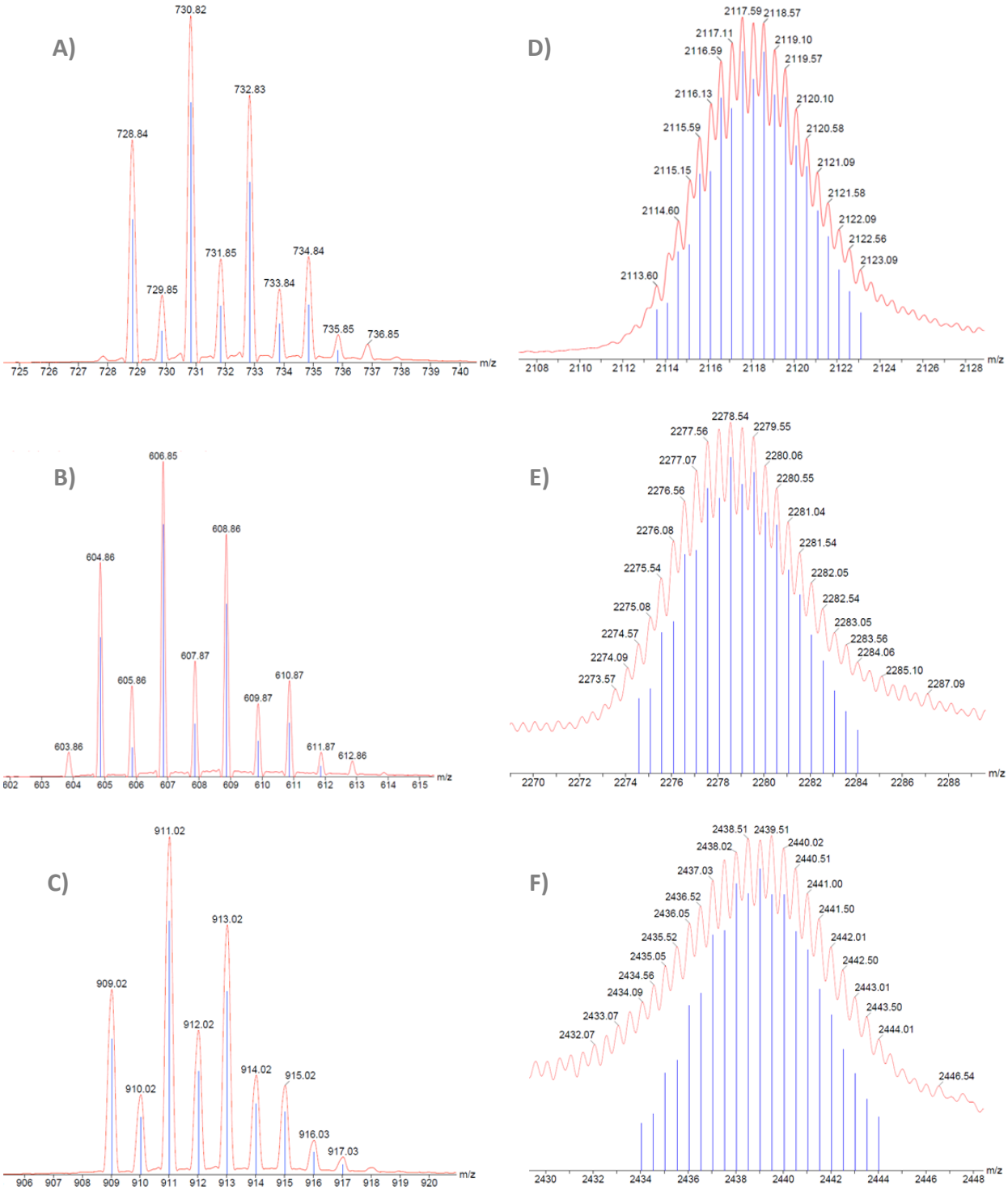

Figure S11. Predicted (blue) and observed (red) isotopic patterns for $[Cu_4O(OH)L_2(NO_3)_2]^-$ (**A**), $[Cu_4O(OH)L_2]^+$ (**B**), $[Cu_4(OH)L_4]^-$ (**C**), $[Cu_{26}(OH)_{26}(L)_{13}(CO_3)]^{2-}$ (**D**), $[Cu_{28}(OH)_{28}(L)_{14}(CO_3)]^{2-}$ (**E**) and $[Cu_{30}(OH)_{30}(L)_{15}(CO_3)]^{2-}$ (**F**).

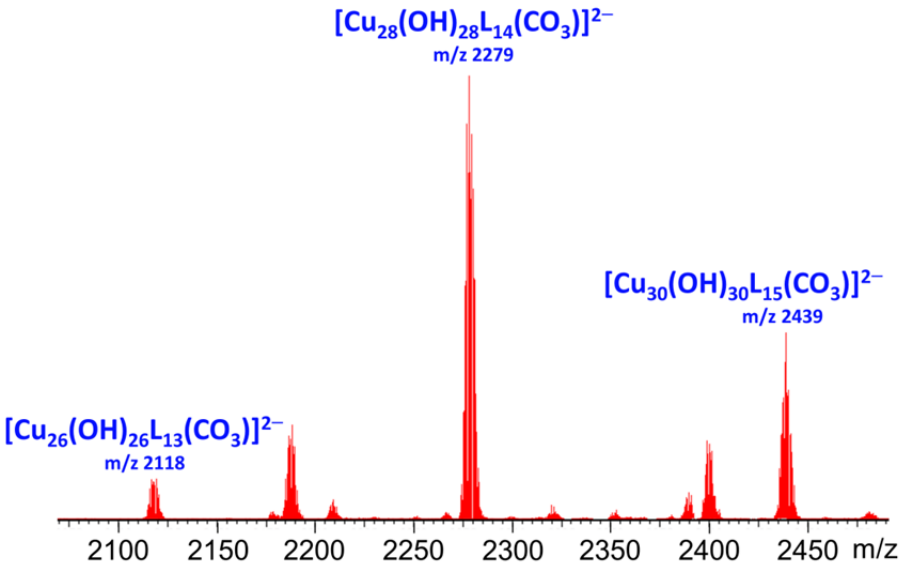

Figure S12. ESI-MS(−) spectrum (in CH_3CN) of the nanojar mixture dissolved in DMSO-d_6 at 25 °C.

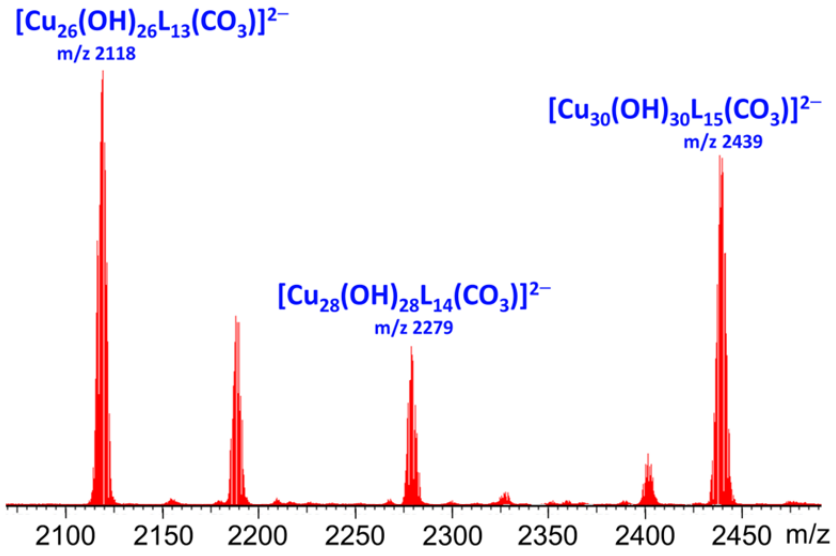

Figure S13. ESI-MS(−) spectrum (in CH_3CN) of the nanojar mixture dissolved in DMSO-d_6 after heating to 70 °C.

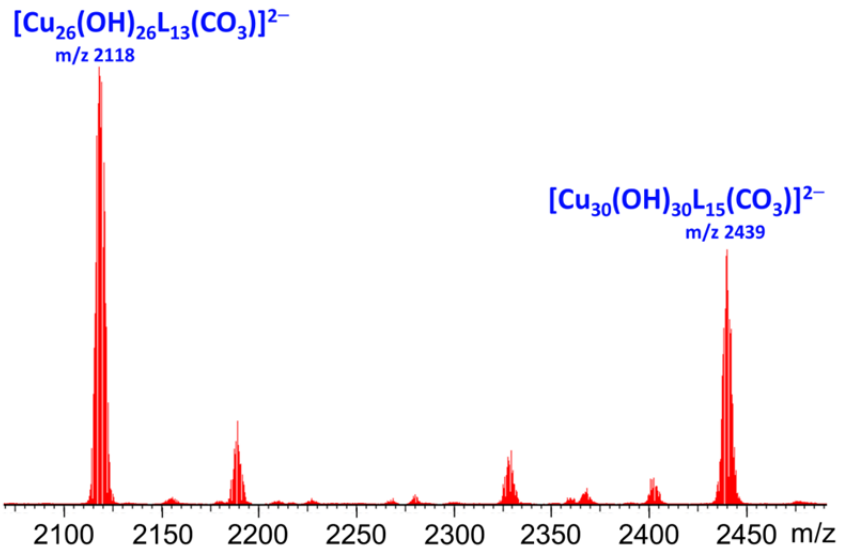

Figure S14. ESI-MS(−) spectrum (in CH_3CN) of the nanojar mixture dissolved in DMSO-d_6 after heating to 110 °C.

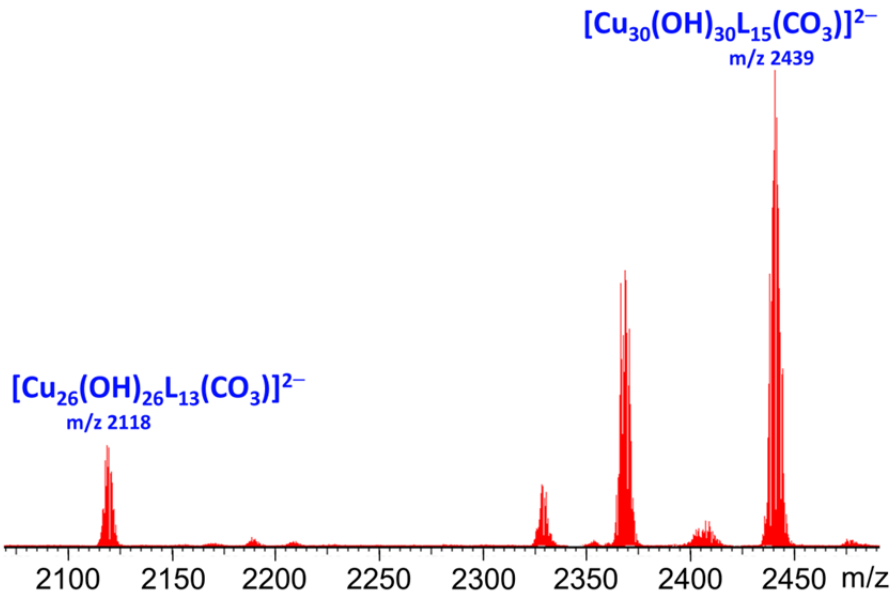

Figure S15. ESI-MS(−) spectrum (in CH_3CN) of the nanojar mixture dissolved in DMSO-d_6 after heating to 150 °C.

7. X-RAY CRYSTALLOGRAPHIC DATA

X-ray quality single-crystals of **7** are grown from an ethyl acetate solution by hexane vapor diffusion. Single-crystals of $\mathbf{LH_2}$ are obtained by slow evaporation of an EtOH/H_2O solution. Single-crystals of **1**$(py)_5$ are obtained by $^{i}Pr_2O$ vapor diffusion to a pyridine solution of **1**$(H_2O)_2(THF)$. Single-crystals of **2** are obtained from CH_2Cl_2 or acetone solution by Et_2O vapor diffusion. X-ray diffraction data are collected at room temperature from a single-crystal mounted atop a glass fiber with cyanoacrylate glue, with a Bruker SMART APEX II diffractometer using graphite-monochromated Mo-Kα (λ = 0.71073 Å) radiation. The structures are solved by employing SHELXTL direct methods and refined by full-matrix least squares on F^2, using the APEX2 v2014.9-0 software package (Bruker AXS Inc.: Madison, WI, 2014). All non-H atoms are refined with independent anisotropic displacement parameters, except the disordered atoms in **2** (one of the two crystallographically independent molecules, and one butyl arm of the tetrabutylammmonium counterion; 50/50), for which geometric restraints are used. C–H hydrogen atoms are placed in idealized positions and refined using the riding model. O–H hydrogen atoms are located from the difference Fourier maps; their displacement parameters are fixed to be 20 % larger than those of the attached O atoms. Crystals of **1**$(py)_5$ were poorly diffracting and only preliminary data are presented here. Table S1 summarizes the crystallographic details; thermal ellipsoid plots are shown in Figures S10−S12, along with a packing diagram of $\mathbf{LH_2}$ showing H-bonding (Fig. S13). Crystallographic data have been deposited at the Cambridge Crystallographic Data Centre (deposition numbers: CCDC 1508663−1508665, 1519412). Copies of the data can be obtained free of charge via http://www.ccdc.cam.ac.uk/conts/retrieving.html (or from the Cambridge Crystallographic Data Centre, 12, Union Road, Cambridge, CB2 1EZ, UK; fax: +44 1223 336033; e-mail: deposit@ccdc.cam.ac.uk).

Table S1. Summary of crystallographic data.

	LH_2	**1**$(py)_5$	**2**	**7**
Formula	$C_8H_{10}N_4$	$C_{41}H_{43}Cu_4N_{15}O_8$	$C_{48}H_{69}Cu_4N_{17}O$	$C_{12}H_{20}N_2O_2$
FW	162.20	1128.06	1154.36	224.30
Crystal system	monoclinic	orthorhombic	monoclinic	monoclinic
Space group	$P2_1/c$	$P2_12_12_1$	$P2_1/c$	C2/c
a/Å	5.57982(8)	11.0383(2)	19.4050(6)	16.6684(3)
b/Å	4.79015(7)	19.3794(5)	13.4239(4)	5.4357(1)
c/Å	15.1644(2)	25.1577(6)	19.5853(6)	14.3613(3)
α/deg	90.000	90.000	90.000	90.000
β/deg	94.0417(8)	90.000	94.268(2)	98.362(1)
γ/deg	90.000	90.000	90.000	90.000
V/Å^3	404.31(1)	5381.6(2)	5087.6(3)	1287.36(4)
Z	2	4	4	4
D_{calc}/g cm^{-3}	1.332	1.392	1.507	1.157
μ/mm^{-1}	0.087	1.618	1.705	0.079
Reflns collected/unique	9615/1021	53884/4281	73685/8533	18079/2348
R(int)	0.0215	0.0624	0.0665	0.0190
Obsd reflns [$I > 2\sigma(I)$]	844	3994	6781	1870
Data/parameters/restrains	1021/58/0	4281/619/21	8533/612/18	2348/75/0
GOF (on F^2)	1.050	1.150	1.092	1.059
R(F), R_w(F) [$I > 2\sigma(I)$]	0.0379, 0.0966	0.0530, 0.1585	0.0787/0.1586	0.0557, 0.1681
R(F), R_w(F) [all data]	0.0472, 0.1027	0.0578/0.1641	0.1004/0.1693	0.1201, 0.1821
Residual peak/hole (e·Å^{-3})	0.185/ −0.165	1.043/−0.358	1.689/−0.973	0.314/ −0.251

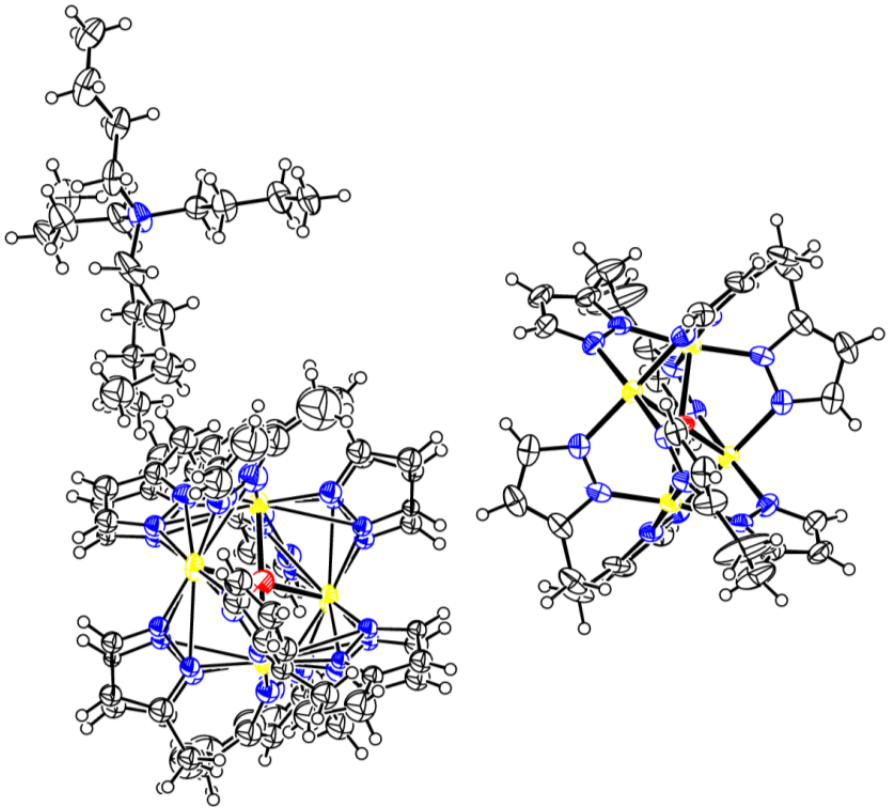

Figure S16. Thermal ellipsoid plot (50% probability) of $(Bu_4N)[Cu_4(\mu_4\text{-}OH)(\mu_3\text{-}L)_4]$ (**2**).

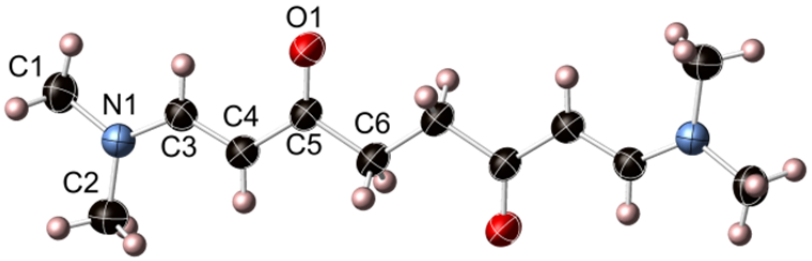

Figure S17. Thermal ellipsoid plot (50%) of the crystal structure of **7**. Bond lengths (Å): C1−N1: 1.447(1); C2−N1: 1.449(2); C3−N1: 1.335(1); C3−C4: 1.363(1); C4−C5: 1.442(2); C5−O1: 1.229(1); C5−C6: 1.517(1); C6−C6*: 1.498(2). Symmetry operator (*): −x+1, −y, −z+1.

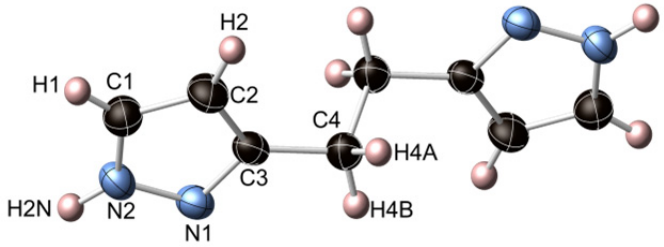

Figure S18. Thermal ellipsoid plot (50%) of the crystal structure of $\mathbf{LH_2}$. Bond lengths (Å): N1−N2: 1.356(1); N2−C1: 1.333(2); C1−C2: 1.369(2); C2−C3: 1.399(2); C3−N1: 1.333(2); C3−C4: 1.497(2); C4−C4*: 1.528(2). Symmetry operator (*): −x, y−1/2, −z+1/2.

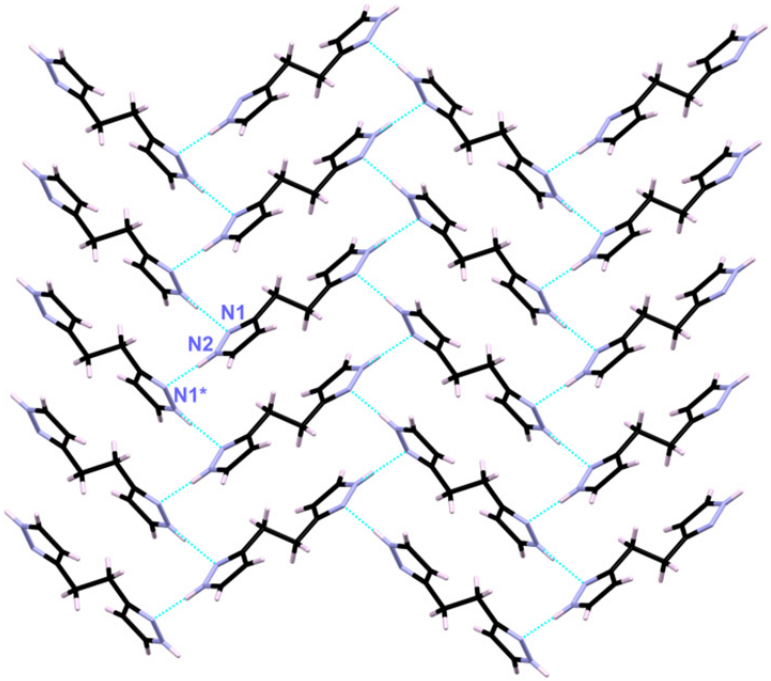

Figure S19. Crystal packing diagram of $\mathbf{LH_2}$. Hydrogen bonding: N2···N1*: 2.923(1) Å; N2−H2N: 0.88(1) Å; H2N···N1*: 2.08(1) Å; N2−H2N···N1*: 159(1) °. Symmetry operator (*): −x, y−1/2, −z+1/2.